AD-763 792

MAGNETO-OPTIC EFFECTS @ 1.15 MICROMETER IN GD(.5)Y(2.5)GA(1) IRON GARNET THIN FILM WAVEGUIDE

Samuel C. Tseng, et al

IBM Thomas J. Watson Research Center

MAGNETO-OPTIC EFFECTS @ 1.15 μm IN Gd$_{.5}$Y$_{2.5}$Ga$_1$ IRON GARNET THIN FILM WAVEGUIDE

Quarterly Technical Report

(15 January 1973-15 April 1973)

June 1973

by

A. R. Reisinger
S. C. Tseng (principal investigator)

Prepared under Contract N00014-73-C-0256

DISTRIBUTION STATEMENT A

Approved for public release;
Distribution Unlimited

by

IBM Corporation
Thomas J. Watson Research Center
P. O. Box 218
Yorktown Heights, New York 10598

D D C
JUL 30 1973
C

MAGNETO-OPTIC EFFECTS @ 1.15 μm IN $Gd_{.5}Y_{2.5}Ga_1$ IRON GARNET THIN FILM WAVEGUIDE

Quarterly Technical Report

(15 January 1973-15 April 1973)

June 1973

by

A. R. Reisinger
S. C. Tseng (principal investigator)

by

IBM Corporation
Thomas J. Watson Research Center
P. O Box 218
Yorktown Heights, New York 10598

ia

TABLE OF CONTENTS

DOCUMENT CONTROL DATA – R & D

(Security classification of title, body of abstract and indexing annotation must be entered when the overall report is classified)

1. ORIGINATING ACTIVITY (Corporate author)	2a. REPORT SECURITY CLASSIFICATION
IBM T. J. Watson Research Center P.O. Box 218 Yorktown Heights, N. Y. 10598	Unclassified
	2b. GROUP

3. REPORT TITLE

Magneto Optic Effects @ 1.15 μm in $Gd_5Y_{2.5}Ga_1$ Iron Garnet Thin Film Waveguides

4. DESCRIPTIVE NOTES *(Type of report and inclusive dates)*

5. AUTHOR(S) *(First name, middle initial, last name)*

Tseng, Samuel C.; Reisinger, Axel R.; Powell, Carl G.
(S. C. Tseng, Principal Investigator)

6. REPORT DATE	7a. TOTAL NO. OF PAGES	7b. NO. OF REFS
June, 1973	36	8

8a. CONTRACT OR GRANT NO.	9a. ORIGINATOR'S REPORT NUMBER(S)
N00014-73-C-0256	
b. PROJECT NO.	
c.	9b. OTHER REPORT NO(S) (Any other numbers that may be assigned this report)
d.	

10. DISTRIBUTION STATEMENT

Approved for public release, distribution unlimited.

11. SUPPLEMENTARY NOTES	12. SPONSORING MILITARY ACTIVITY
	Advanced Research Projects Agency ARPA Order No. 2327

13. ABSTRACT

Two $(Gd_5Y_{2.5})(Fe_4Ga_1)O_{12}$ garnet films deposited on GGG substrates have been tested for possible use as modulators, switches and isolators. Their passive optical waveguiding properties have been characterized at a wavelength of 1.15 μm. Modulation of the output, passed through an analyzer, was observed by applying a longitudinal magnetic field. The mode conversion efficiency was shown to be limited primarily by the phase velocity mismatch between TE and TM modes. The possibility of phase modulation of TM modes by a transverse magnetic field is discussed in the light of data obtained in the mode conversion experiments.

DD FORM 1473
1 NOV 65

KEY WORDS	LINK A		LINK B		LINK C	
	ROLE	WT	ROLE	WT	ROLE	WT
Magneto-Optics						
Garnet Films						
Optical Waveguides						
Modulation						
Mode Conversion						

I. INTRODUCTION

Mode conversion due to non-zero off-diagonal elements in the dielectric tensor has been demonstrated in anisotropic[1,2] as well as magneto-optic[3] waveguides. Because the coupling efficiency can be conveniently influenced by external means, namely application of a magnetic field, magneto-optic structures enjoy intrinsic superiority over their anisotropic counterparts with a view toward active devices.

The pertinent theoretical framework is briefly outlined in Section II. In the presence of a longitudinal magnetic field, the normal modes are admixtures of (uncoupled) TE and TM modes,[4] resulting in mode conversion, similar to the Faraday effect in bulk media. With a transverse magnetic field, pure TE and TM modes continue to exist. The propagation constant of the latter depends on the off-diagonal dielectric constant δ. For modes far from cutoff, the dependence is quadratic and can be assimilated to the conventional Voigt effect. By contrast, it is linear for modes near cutoff. With no preconceived idea about the magnitude of δ, the possibility of phase modulating TM modes is raised.

Against this backdrop, we have tested two $(Gd_{.5}Y_{2.5})$ $(Fe_4Ga)O_{12}$ garnet films grown on GGG substrates at our laboratory for possible use as modulators, switches and isolators. Preliminary experimental results are presented in Section III. The passive optical waveguiding properties have been characterized at a wavelength of 1.152 μm. Our data relative to TE$\rightleftarrows$TM mode conversion induced by a longitudinal magnetic field can

be interpreted satisfactorily with existing theories. The effect
of a transverse field is somewhat unclear at the present time.

II. THEORETICAL BACKGROUND

2.1 Mode Conversion

Consider an optical waveguiding structure, illustrated in Fig. 1, where the z-axis is chosen as the propagation direction of the guided modes. If one assumes that the film is made of a magneto-optic material, its optical properties in the presence of a longitudinal (along the z-axis) magnetic field are described by the following dielectric tensor:

$$||\epsilon_F|| = \epsilon_0 \begin{bmatrix} \epsilon_F & j^\delta & 0 \\ -j^\delta & \epsilon_F & 0 \\ 0 & 0 & \epsilon_F \end{bmatrix} \tag{1}$$

where the film is assumed to be optically isotropic in the absence of a magnetic field. Coupling between TE and TM modes occurs via the off-diagonal elements in eq. (1),[4] resulting in mode conversion which has been demonstrated by Tien et al.[3] This phenomenon is similar to the Faraday rotation in isotropic bulk media. In waveguides, however, even if all materials involved are isotropic, TE and TM modes travel with different phase velocities. If the electric field is originally polarized in the y-direction (TE mode) the amplitude conversion efficiency, derived on the basis of coupled mode theory, is given by:[2]

$$R(z) = \frac{E_x(z)}{E_y(z)} = (1 + B^2)^{-1/2} \quad \sin\left[Kz \ (1 + B^2)^{1/2} \right] \tag{2}$$

where K is the "coupling strength" and $B = \Delta\beta/2K$ is proportional to the

mismatch $\Delta\beta$ between the propagation constants of TE and TM modes. By making $\Delta\beta = 0$ in eq. (2), it is clear that the "coupling strength" K is equal to the optical rotatory power α of the magneto-optic material, which is itself related to the magnitude of the off-diagonal term δ in eq. (1) by the following expression:[3]

$$K = \alpha = \frac{\pi}{\lambda_0\, n_F}\; \delta \tag{3}$$

where λ_0 is the vacuum wavelength of the incident light and n_F is the refractive index of the magneto-optic film. Only in the case of perfect phase matching ($\Delta\beta = 0$) can the conversion be 100% efficient.

2.2 Phase Modulation

Let us assume that the magnetic field is now applied along the y direction (transverse configuration). The dielectric tensor representing the optical properties of the film reads in this case:

$$\lVert \epsilon \rVert = \epsilon_0 \begin{bmatrix} \epsilon_F & 0 & j\delta \\ 0 & \epsilon_F & 0 \\ -j\delta & 0 & \epsilon_F \end{bmatrix} \tag{4}$$

It is shown in the Appendix that, unlike the previous case, pure, uncoupled, TE and TM modes can propagate. TE modes are, in fact, completely unaffected by the applied transverse magnetic field, whereas the propagation constant of TM modes does depend on the off-diagonal element δ through the following transcendental equation:

$$q_F\ w = \tan^{-1}\left[\frac{(p_s/\epsilon_s)+a}{b}\right] + \tan^{-1}\left[\frac{(p_T/\epsilon_T)-a}{b}\right] + N\pi \qquad (5)$$

The various parameters appearing in eq. (5) are defined as follows:

$$q_F^2 = k_0^2\ \epsilon_F\ [\ 1 - (\delta/\epsilon_F)^2] - \beta^2 \qquad (6a)$$

$$p_s = \beta^2 - k_0^2\ \epsilon_s \qquad (6b)$$

$$p_T = \beta^2 - k_0^2\ \epsilon_T \qquad (6c)$$

$$a = (\beta\delta/\epsilon_F^2)\ [\ 1 - (\delta/\epsilon_F)^2\ ]^{-1} \qquad (6d)$$

$$b = (q_F/\epsilon_F)\ [\ 1 - (\delta/\epsilon_F)^2\ ]^{-1} \qquad (6e)$$

w = waveguide thickness

β = guided mode propagation constant

k_0 = free-space propagation constant

ϵ_s, ϵ_F, ϵ_T = isotropic dielectric constants of the substrate, film and top (surrounding medium), respectively.

N = mode order = 0, 1, 2, 3, ...

It is easily verified that when $\delta = 0$, eq. (5) reduces to the familiar form. For modes well above cutoff, $q_F \to 0$, and eq. (6a) gives an approximate expression for the propagation constant:

$$\beta^2 \simeq k_0^2 \; \epsilon_F \; [\; 1 - (\delta/\epsilon_F)^2 \;] \tag{7}$$

β does not depend on the sign of the off-diagonal element δ. This is the conventional Voigt effect, also commonly referred to as linear magnetic birefringence.

For modes near cutoff, on the other hand, $p_s \to 0$ and $\beta^2 \simeq k_0^2 \; \epsilon_s$. The waveguide equation (5) can be approximated by:

$$q_F \; w \simeq \frac{a}{b} + \tan^{-1} \left[\frac{\epsilon_F}{\epsilon_T} \; \frac{p_T}{q_F} \right] + N\pi$$

which depends linearly on δ via eq. (6d). Table I shows how the guided index $n_g = \beta/k_0$ changes with the sign and magnitude of the off-diagonal element δ for TM modes of order 9 (near cutoff) and 0 (far from cutoff), respectively. The pertinent waveguide parameters were chosen as follows: film thickness = 6.4 μm, film index = 2.14, substrate index = 1.95, air as surrounding medium, and λ_0 = 1.15 μm. Notice that the changes Δn_g, although small, are roughly two orders of magnitude larger for modes near cutoff than for their counterparts well above cutoff. The approximately linear dependence of Δn_g on δ is of potential interest for nonreciprocal devices.

III. EXPERIMENTAL RESULTS

3.1 Garnet Films

We have tested two films (hereafter referred to as Sample A and Sample B) of $(Gd_{.5}Y_{2.5})$ $(Fe_4G_a)O_{12}$ deposited by liquid phase epitaxy on (111) GGG substrates, with the magnetization lying in the plane of the film. B-H curves, such as the one shown in Fig. 2, yield the magnitude of the magnetization. $4\pi M$ was measured to be 200G for Sample A, and 175G for Sample B.

The passive waveguiding properties of these films were evaluated using the 1.152 μm radiation from a He/Ne laser. Input and output grating couplers were fabricated using the conventional technique.[5] The samples were mounted vertically on a rotating stage, as illustrated schematically in Fig. 3. Although no visible streak of light could be detected through an infrared viewer, indicating surprisingly low surface scattering losses, excitation of guided modes was evidenced by the observation of "m-lines"[6] emerging from the output grating. The best fit between experimental and theoretical values of the guided index n_g was obtained with a substrate index of 1.95, a film index of 2.135, and a film thickness of 8.4 μm and 6.35 μm for samples A and B, respectively. Since their phase velocities are not very different, TE and TM modes of the same order can be excited simultaneously by a converging incoming beam polarized at 45°. This allows direct determination of the mismatch $\Delta n_g = n_g^{TE} - n_g^{TM}$ by measuring the angular separation of the two outputs. Experimental data, shown in Fig. 4 for various mode orders N, are in good agreement with theory.

3.2 Mode Conversion With Longitudinal Field

Assuming that the optical wave is originally polarized in the y-direction (E_y corresponding to TE modes), application of a longitudinal magnetic field will convert some amount of light to the perpendicular polarization E_x. When the output is passed through an analyzer, as illustrated in Fig. 3, with azimuth Θ relative to the original polarization direction, the intensity detected is, in a simplified analysis, given by:

$$I_D = E_y^2 \cos^2\Theta + E_x^2 \sin^2\Theta + E_x E_y \cos\phi \sin 2\Theta \qquad (8)$$

where ϕ is the phase difference between E_x and E_y after traversing the waveguide. Conservation of energy imposes the condition $E_y^2 + E_x^2 = I_0 = $ constant. Thus:

$$(I_D/I_0) = \cos^2\Theta + (E_x/E_y)^2 (\sin^2\Theta - \cos^2\Theta) + (E_x/E_y) \cos\phi \sin 2\Theta \qquad (9)$$

A longitudinal AC magnetic field $H_L = H_0 \cos\Omega t$ was applied at a frequency of 60 Hz by means of a Helmholtz coil. The coupling strength K, proportional to the off-diagonal element δ by virtue of eq. (3), is such that $K(-H_L) = -K(H_L)$. Hence, it follows from eq. (2) that (E_x/E_y) contains the frequencies Ω, 3Ω, etc., while the lowest frequency in the $(E_x/E_y)^2$ term is 2Ω. The DC term and the 60 Hz

modulated signal do depend on the analyzer azimuth as $\cos^2\theta$ and $\sin2\theta$ respectively, as evidenced in Fig. 5. Fig. 6 confirms that, after processing the signal through an electronic filter, the 60 Hz component is proportional to the H_L with maximum slope at $\theta = 45°$, while the 120 Hz component varies as $-H^2$ when $\theta = 0$. The observation of the 60 Hz modulated signal, arising from the cross term in eq. (8), was somewhat unexpected since, as noted earlier, TE and TM modes are coupled out at slightly different angles. However, the angular spectra of the outputs are not infinitely sharp and interference probably occurs in the overlap region.

In the case of large mismatch $\Delta\beta$ or weak coupling K (B >> 1), eq. (2) simplifies to take on the form:

$$E_x/E_y \simeq (2K/\Delta\beta) \sin (\Delta\beta\ z/2) \tag{10}$$

When $\theta = 45°$ and assuming B >> 1, the 60 Hz signal modulation ratio, obtained from eq. (9), can be approximated by:

$$\eta(z) = (2K/\Delta\beta) \sin (\Delta\beta\ z)$$

In this last expression, we have made use of the fact that, when B >> 1, the phase difference ϕ between TE and TM modes is approximately equal to $(\Delta\beta\ z)/2$.[7] Because the quantity $(\Delta\ell\ z)$ typically covers one spatial period over the size of the output grating, the

detector sees an average of $| \overline{\sin(\Delta\beta\ z)} | \simeq 0.65$. The modulation ratio detected is:

$$\overline{\eta} = 1.3K/\Delta\beta \tag{11}$$

Experimental data plotted in Fig. 7 confirms that the modulation ratio at 60 Hz is inversely proportional to $\Delta n_g = \Delta\beta/k_0$. This observation is offered as additional evidence that we are indeed looking at the cross term in eq. (8). From the slope of the straight line in Fig. 7 we obtain an approximate value for the optical rotation K of 240°/cm, which appears to be a reasonable estimate.[3, 8] On the basis of this figure, the off-diagonal element δ should be, by virtue of eq. (3), on the order of 3×10^{-4}. Also, the TE → TM conversion efficiency between crossed polarizer and analyzer is expected to be $\sim 1.1\%$ for the mode-order N = 3. The experimental value was measured to be $\sim 0.8\%$.

3.3 Amplitude Modulation with Longitudinal Field

In the experiment discussed above, the 60 Hz modulated signal due to longitudinal magnetic field disappeared for an analyzer azimuth of 0° or 90°. We observed that this signal could be made to reappear with unexpectedly large magnitude by simultaneously exciting TE and TM modes of the same order. In contrast to the previous case, the modulated intensity no longer varies with the analyzer azimuth Θ as sin 2Θ. Thus, it cannot arise from the cross term in eq. (8). Instead, we ascribe it to amplitude modulation of the E_x^2 and E_y^2 terms.

The waveguide can be thought of, in a simple way, as a bire-fringent magneto-optic crystal. The electric field, after traversing a distance L of the crystal, is given in terms of E_x^0 and E_y^0 at the input by the following matrix relation:

$$\begin{bmatrix} E_x \\ E_y \end{bmatrix} = \begin{bmatrix} a^* & -b \\ +b & a \end{bmatrix} \begin{bmatrix} E_x^0 \\ E_y^0 \end{bmatrix} \tag{12}$$

where the coefficient b is proportional to the off-diagonal element δ, and therefore contains the frequency Ω of the applied magnetic field, while a and a^* contain frequencies that are even multiples of Ω. It follows from eq. (12) that:

$$|E_x|^2 = |a|^2 E_x^{0^2} + b^2 E_y^{0^2} - b (a+a^*) E_x^0 E_y^0$$

$$|E_y|^2 = b^2 E_x^{0^2} + |a|^2 E_y^{0^2} + b (a+a^*) E_x^0 E_y^0 \tag{13}$$

Notice that the last terms in eqs. (13) involve the product $E_x^0 E_y^0$. Thus simultaneous excitation of TE and TM modes is necessary. The photographs displayed in Fig. 8, corresponding to equal excitation of TE and TM modes of order 9 in Sample B, show that TE and TM outputs are modulated with approxmately the same amplitude and opposite phases, as expected on the basis of eq. (13). The modulation depth, defined as the ratio of the 60 Hz and DC components, was 6.5%, significantly larger than the mode conversion efficiency.

3.4 Effect of a Transverse Field

In another experiment, an AC transverse magnetic field at 60 Hz was superimposed to a DC longitudinal field. Fig. 9 shows the behavior displayed by Sample A, between crossed polarizer and analyzer, for the mode order 4. Both fields were required in order for the output to be modulated. Note that if the only effect of the AC field was to rotate the magnetization in the plane of the film, the observed modulation frequency would be 120 Hz, rather than 60 Hz. Our original explanation was that we had achieved modulation of the conversion efficiency by varying the mismatch Δn_g between TE and TM modes, as discussed in Section 2.2. However, the variation of Δn_g required to account for the observed modulation amplitude is of the order of 5×10^{-5}, which would imply, based on Table I, an off-diagonal element δ in the range 10^{-2} to 10^{-1}. This is hardly reconcilable with our estimate of 3×10^{-4} arrived at in connection with our mode conversion experiments, and it appears now unlikely that our initial interpretation was correct. Furthermore, the phenomenon just described was not observed in Sample B. In the latter case, the output was modulated even in the absence of a DC longitudinal field. Although we do not, at the present time, have a clear understanding of these features, we feel that they might possibly be attributable to the fact that rotation of the magnetization is not quite isotropic in the plane of the film, as is apparent in Fig. 2 (the two B-H curves correspond to orthogonal directions). Experimentation is currently in progress to attempt to clarify this point.

IV. CONCLUSION

During this reporting period, we have shown that garnet films available at our laboratory are suitable for magneto-optic work at 1.152 μm. Modulation of optical guided waves by application of longitudinal and transverse magnetic fields has been investigated experimentally in two samples. The basic features of the experimental data pertaining to the longitudinal configuration are now well understood. Various schemes designed to artificially phase match TE and TM modes are currently being considered in order to enhance the mode conversion efficiency which is now limited to about 1%.

Phase modulation by transverse magnetic field, which emerged from a theoretical analysis as of potential interest for nonreciprocal devices, appears now to be too small an effect for practical use, at least in the films that we have tested so far. Alternative solutions are under investigation.

REFERENCES

1) M. Shah, J. D. Crow and S. Wang, "Optical Waveguide Mode-Conversion Experiments," Appl. Phys. Lett., 20, No. 2 (15 Jan. 1972), p. 66.

2) T. P. Sosnowski and H. P. Weber, "Polarization Conversion of Light in Thin-Film Waveguides," Optics Commun., 7, No. 1, (Jan. 1973), p. 47.

3) P. K. Tien, R. J. Martin, R. Wolfe, R. C. LeCraw and S. L. Blank, "Switching and Modulation of Light in Magneto-Optic Waveguides of Garnet Films," Appl. Phys. Lett., 21, No. 8 (15 Oct. 1972), p. 394.

4) S. Yamamoto, Y. Koyamada and T. Makimoto, "Normal-Mode Analysis of Anisotropic and Gyrotropic Thin-Film Waveguides for Integrated Optics," J. Appl. Phys., 43, No. 12 (Dec. 1972), p. 5090.

5) M. L. Dakss, L. Kuhn, P. F. Heidrich & B. A. Scott, "Grating Coupler for Efficient Excitation of Optical Guided Waves in Thin Films," Appl. Phys. Lett., 16, No. 12, (15 June, 1970), p. 523.

6) P. K. Tien, R. Ulrich and R. J. Martin, "Modes of Propagating Light Waves in Thin Deposited Semiconductor Films," Appl. Phys. Lett. 14, No. 9 (1 May 1969), p. 291.

7) W. J. Tabor and F. S. Chen, "Electromagnetic Propagation through Materials Possessing Both Faraday Rotation and Birefringence: Experiments with Ytterbium Orthoferrite," J. Appl. Phys., 40, No. 7, (June 1969) p. 2760.

8) B. Johnson, "The Faraday Effect at Near Infrared Wavelengths in Rare-Earth Garnets," Brit. J. Appl. Phys., 17, (1966), p. 1441.

APPENDIX

Consider an isotropic magneto-optic film surrounded by low index
isotropic claddings. With reference to the coordinate system of Fig. 1,
propagation of a guided mode along the z-direction must obey Maxwell's
curl equations in all regions. In the presence of an applied
transverse magnetic field, these equations have the following form
in the film:

$$- \partial H_y / \partial z = - j \, \omega \, \epsilon_0 \, [\, \epsilon E_x + \epsilon_{13} \, E_z \,] \qquad \text{(A-1a)}$$

$$(\partial H_x / \partial z) - (\partial H_z / \partial x) = - j \, \omega \, \epsilon_0 \, \epsilon E_y \qquad \text{(A-1b)}$$

$$\partial H_y / \partial x = - j \, \omega \, \epsilon_0 \, [\, \epsilon_{31} \, E_x + \epsilon E_z] \qquad \text{(A-1c)}$$

$$- \partial E_y / \partial z = j \, \omega \mu_0 \, H_x \qquad \text{(A-1d)}$$

$$(\partial E_x / \partial z) - (\partial E_z / \partial x) = j \, \omega \mu_0 \, H_y \qquad \text{(A-1e)}$$

$$\partial E_y / \partial x = j \, \omega \mu_0 \, H_z \qquad \text{(A-1f)}$$

with $\epsilon_{13} = j \delta$, $\epsilon_{31} = \epsilon_{13}^* = - j \delta$ and $\epsilon =$ diagonal element.
The above system of equations breaks up into two decoupled sets
involving $(E_y; H_x, H_z)$ on one hand and $(H_y; E_x, E_z)$ on the other.
Eqs. (A-1b), (A-1d) and (A-1f) show that TE modes are completely
unaffected by the non-zero off-diagonal element ϵ_{13}. The remaining three
equations, pertaining to TM modes, can be combined into a propagation
equation in the film:

$$\frac{\partial^2 H_y}{\partial z^2} + \frac{\partial^2 H_y}{\partial x^2} + k_0^2 \, \epsilon_F \, [\, 1 - (\delta/\epsilon_F)^2 \,] \, H_y = 0 \qquad (A-2)$$

whose solution H_y must be of the form:

$$H_y = [\, A \, e^{jq_F x} + B \, e^{-jq_F x} \,] \, e^{j(\omega t - \beta z)} \text{ for } 0 \leq x \leq w \qquad (A-3)$$

Substituting this last expression into eq. (A-2) gives a relation between transverse and longitudinal wavevectors q_F and β:

$$q_F^2 = k_0^2 \, \epsilon_F \, [\, 1 - (\delta/\epsilon_F)^2 \,] - \beta^2 \qquad (A-4)$$

Outside the film the wave is evanescent:

$$H_y = (A+B) \, e^{\, p_s x} \, e^{\, j(\omega t) - \beta z)} \text{ for } x < 0$$

$$\qquad (A-5)$$

$$H_y = (A \, e^{\, jq_F w} + B \, e^{-jq_F w}) \, e^{-p_T(x-w)} \, e^{\, j(\omega t - \beta z)} \text{ for } x > w$$

The claddings are non-magnetic and the decay constants p_s and p_T are defined in the usual manner:

$$p_s^2 = \beta^2 - k_0^2 \, \epsilon_s$$

$$p_T^2 = \beta^2 - k_0^2 \, \epsilon_T$$

The dispersion equation is obtained by ensuring the continuity of tangential electric and magnetic fields, namely H_y and E_z. Contunuity of H_y, as defined in eqs. (A-3) and (A-5) has already been taken care of. From eqs. (A-1a) and (A-1c) we obtain:

$$
-j\omega \epsilon_0 E_z =
\begin{cases}
\left[\epsilon \dfrac{\partial H_y}{\partial x} - \beta \delta H_y \right] \left[\epsilon^2 - \delta^2 \right]^{-1} & \text{in the film} \\[3mm]
\dfrac{1}{\epsilon} \dfrac{\partial H_y}{\partial x} & \text{outside}
\end{cases}
$$

With the help of eqs. (A-3) and (A-5), expressing the continuity of E_z across the boundaries at $x = 0$ and $x = w$ leads to the following system of equations:

$$
A \left[(p_S / \epsilon_S) + a - jb \right] + B \left[(p_S / \epsilon_S) + a + jb \right] = 0
$$

$$(A-6)$$

$$
A \, e^{jq_F w} \left[(-p_T / \epsilon_T) + a - jb \right] + B \, e^{-jq_F w} \left[(-p_T / \epsilon_T) + a + jb \right] = 0
$$

where a and b are defined by:

$$
a = \frac{\beta \delta}{\epsilon_F^2 - \delta^2}
$$

$$
b = \frac{q_F \, \epsilon_F}{\epsilon_F^2 - \delta^2}
$$

The system of eqs. (A-6) has a non-trivial solution where the determinant of the coefficients of A and B is equal to zero. Expanding this determinant leads to the following dispersion equation:

$$q_F \, w = \tan^{-1} \left[\frac{(p_s / \varepsilon_s) + a}{b} \right] + \tan^{-1} \left[\frac{(p_T / \varepsilon_T) - a}{b} \right] + N\pi$$

δ	Δn_g	
	$N = 9$	$N = 0$
-10^{-1}	1.4×10^{-5}	-5.1×10^{-4}
-10^{-2}	4.4×10^{-5}	-4.7×10^{-6}
-10^{-3}	4.8×10^{-6}	-1.1×10^{-8}
-10^{-4}	4.9×10^{-7}	3.5×10^{-9}
-10^{-5}	4.9×10^{-8}	3.9×10^{-10}
10^{-5}	-4.9×10^{-8}	-4.1×10^{-10}
10^{-4}	-4.9×10^{-7}	-4.5×10^{-9}
10^{-3}	-4.9×10^{-6}	-9.1×10^{-8}
10^{-2}	-5.3×10^{-5}	-5.5×10^{-6}
10^{-1}	-9.6×10^{-4}	-5.1×10^{-4}

TABLE I

Fig. 1. Optical waveguide coordinate system.

Fig. 2. Hysterisis curve of sample B in two orthogonal directions.

Fig. 3. Schematic experimental setup.

Fig. 4. Guided index mismatch between TE and TM modes vs mode order.

Fig. 5. Detected intensities (sample B) vs analyzer azimuth θ. The DC and 60-Hz signals vary as $\cos^2 \theta$ and $|\sin 2\theta|$, respectively.

Fig. 6. Oscilloscope displays of signal vs applied field. Unfiltered signal (a); signal filtered at 60 Hz (b) and 120 Hz (c).

Fig. 7. 60-Hz modulation ratio vs mismatch in sample B. The analyzer azimuth is set at 45°.

Fig. 8. Amplitude modulation (upper trace) of TE and TM outputs with longitudinal AC magnetic field (lower trace), with simultaneous excitation of TE and TM modes at the input. TE (a) and TM (b) modulations have comparable amplitudes and opposite phases.

Fig. 9. Modulated signal (upper trace) in sample A with DC longitudinal field of 7.2 G and AC transverse field (lower trace) of 1.3 G. The signal disappears upon turning off either the AC field (b) or the DC field (c).
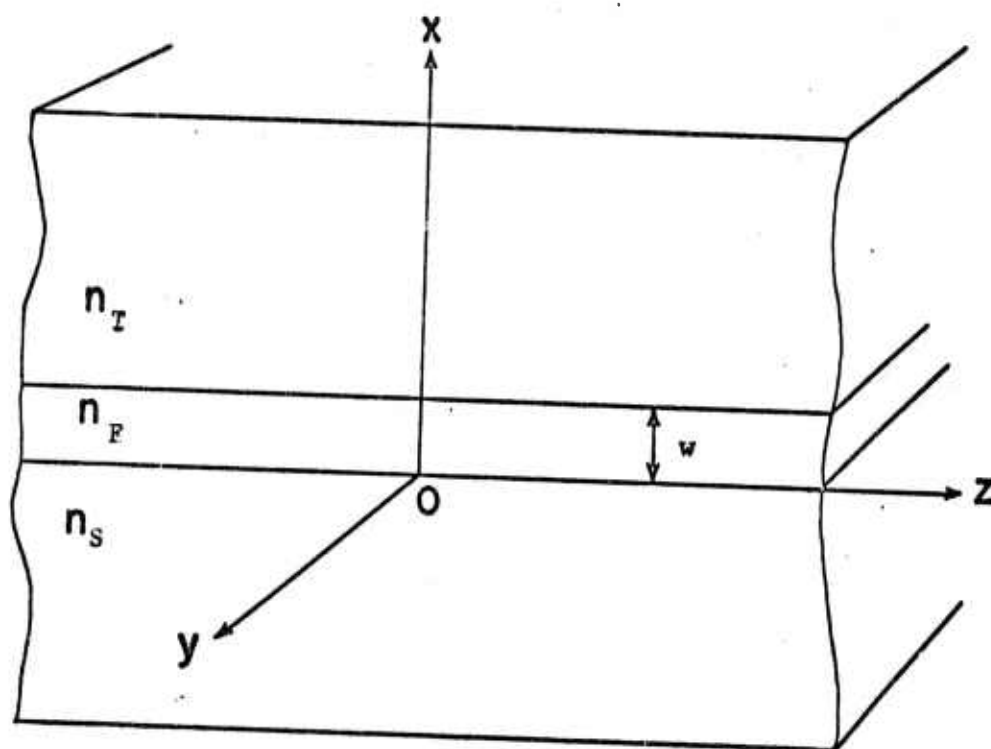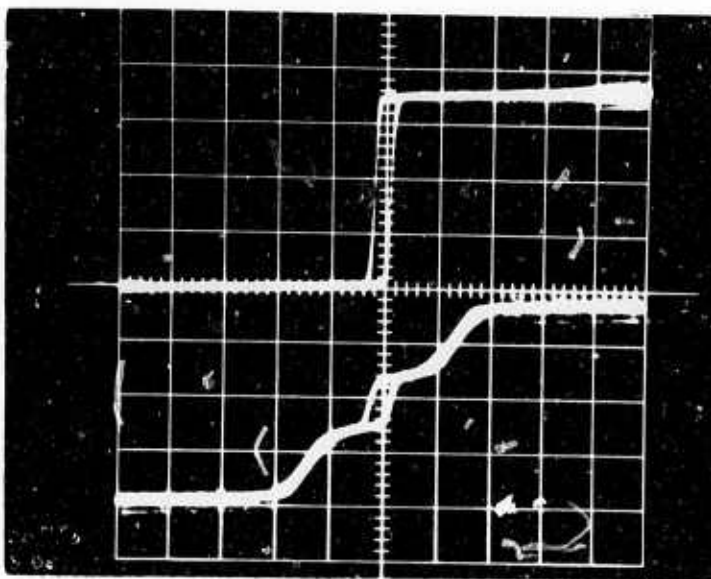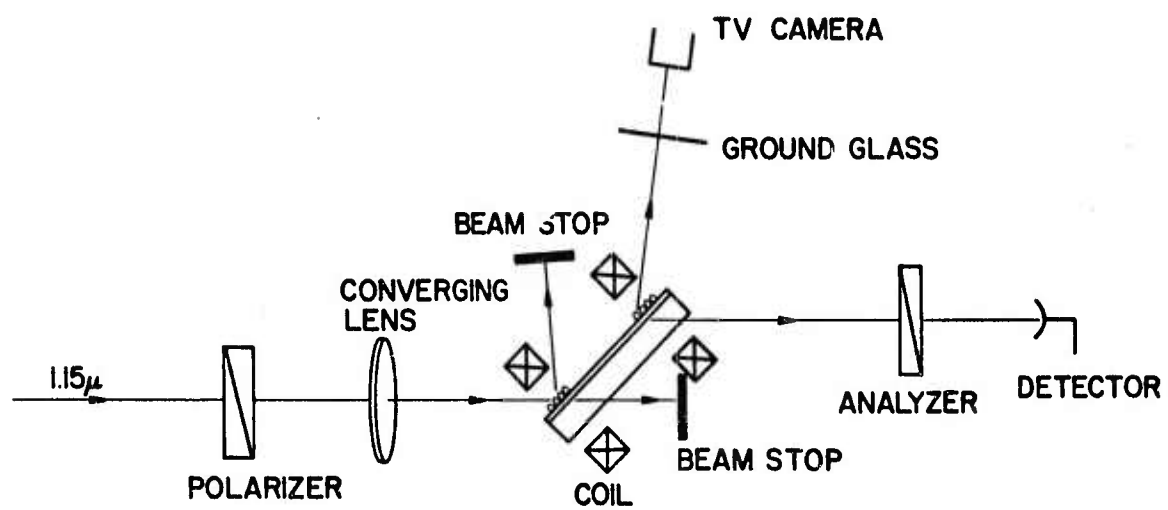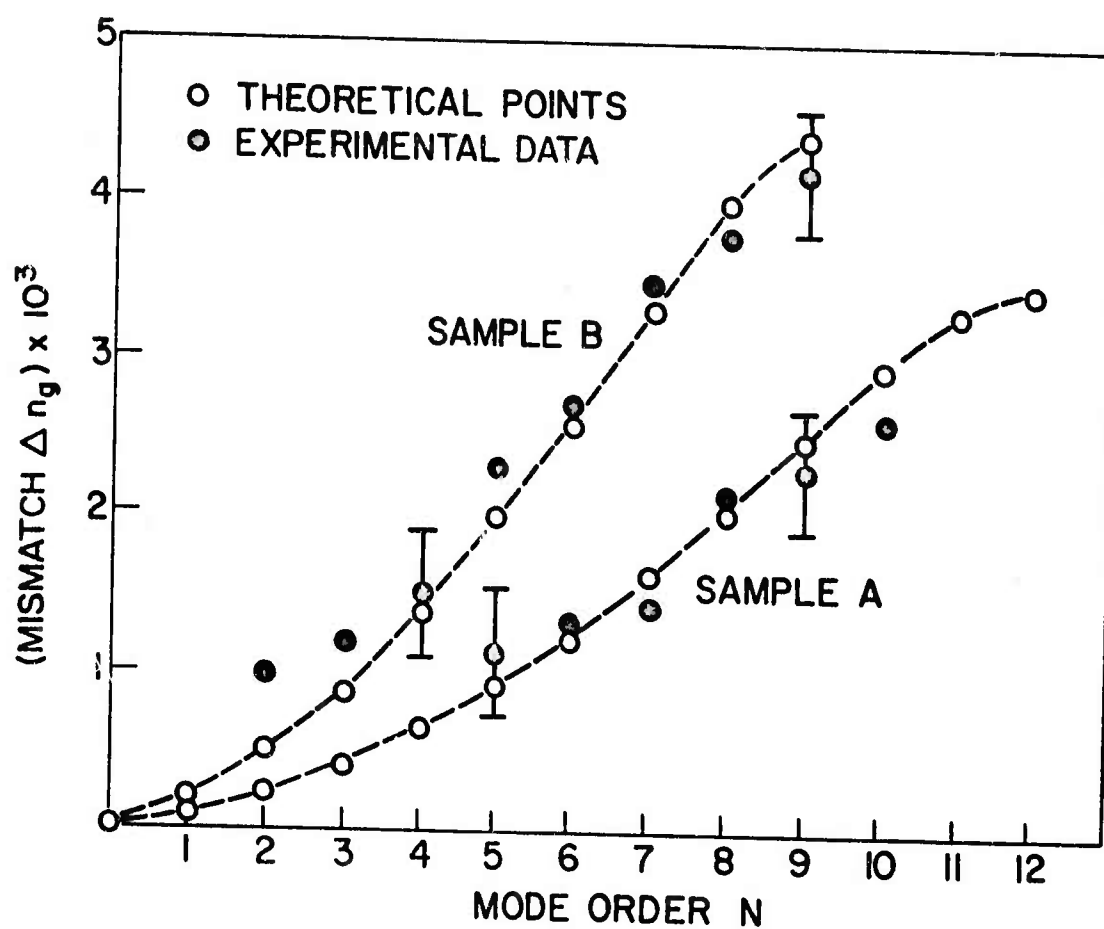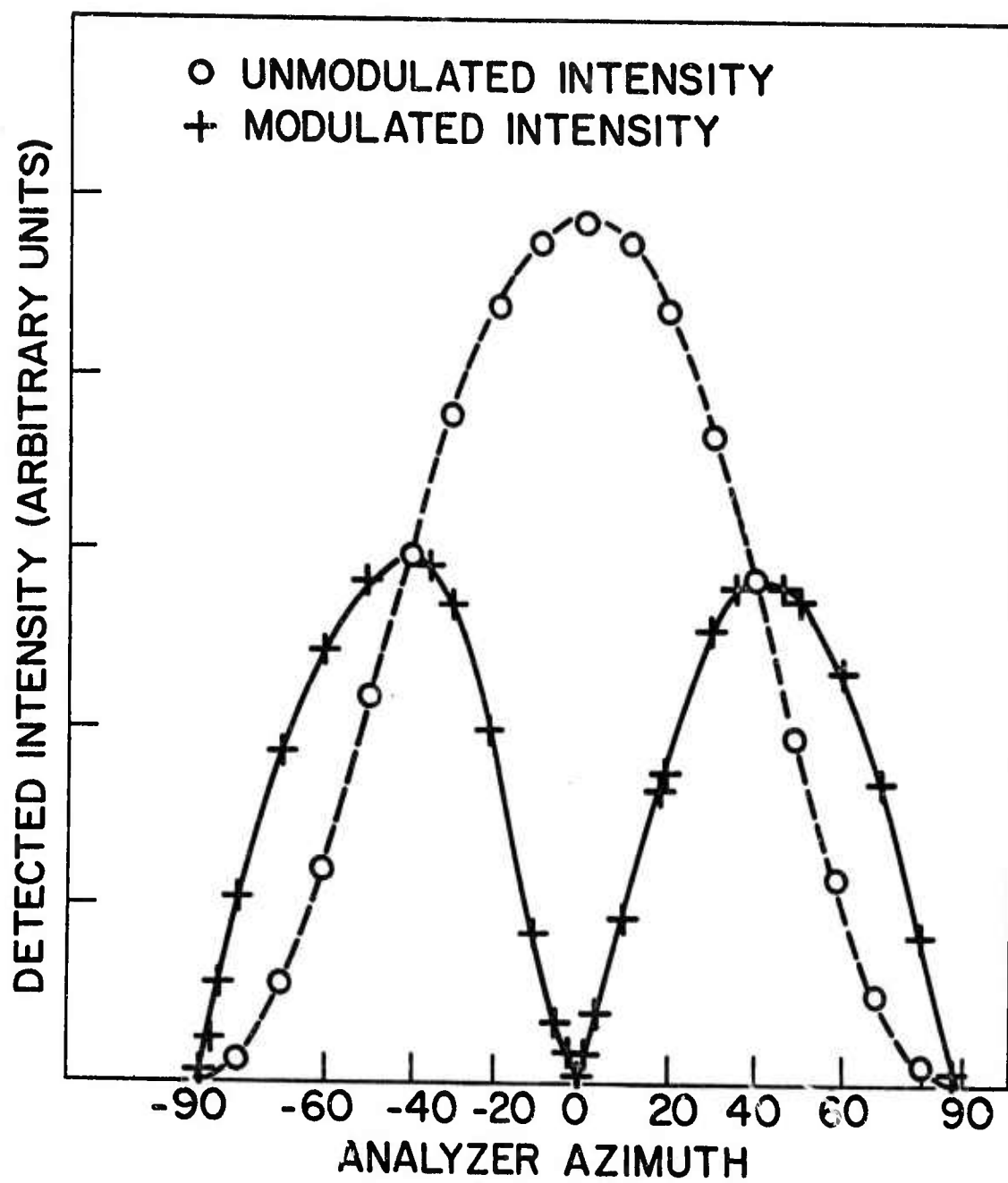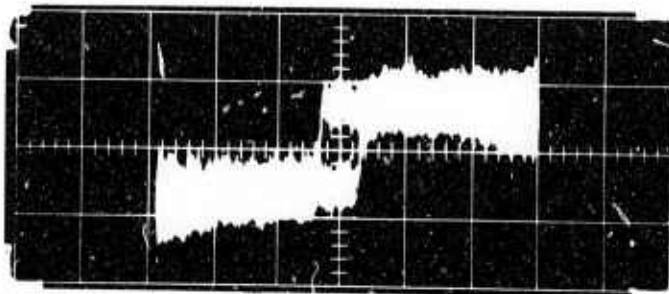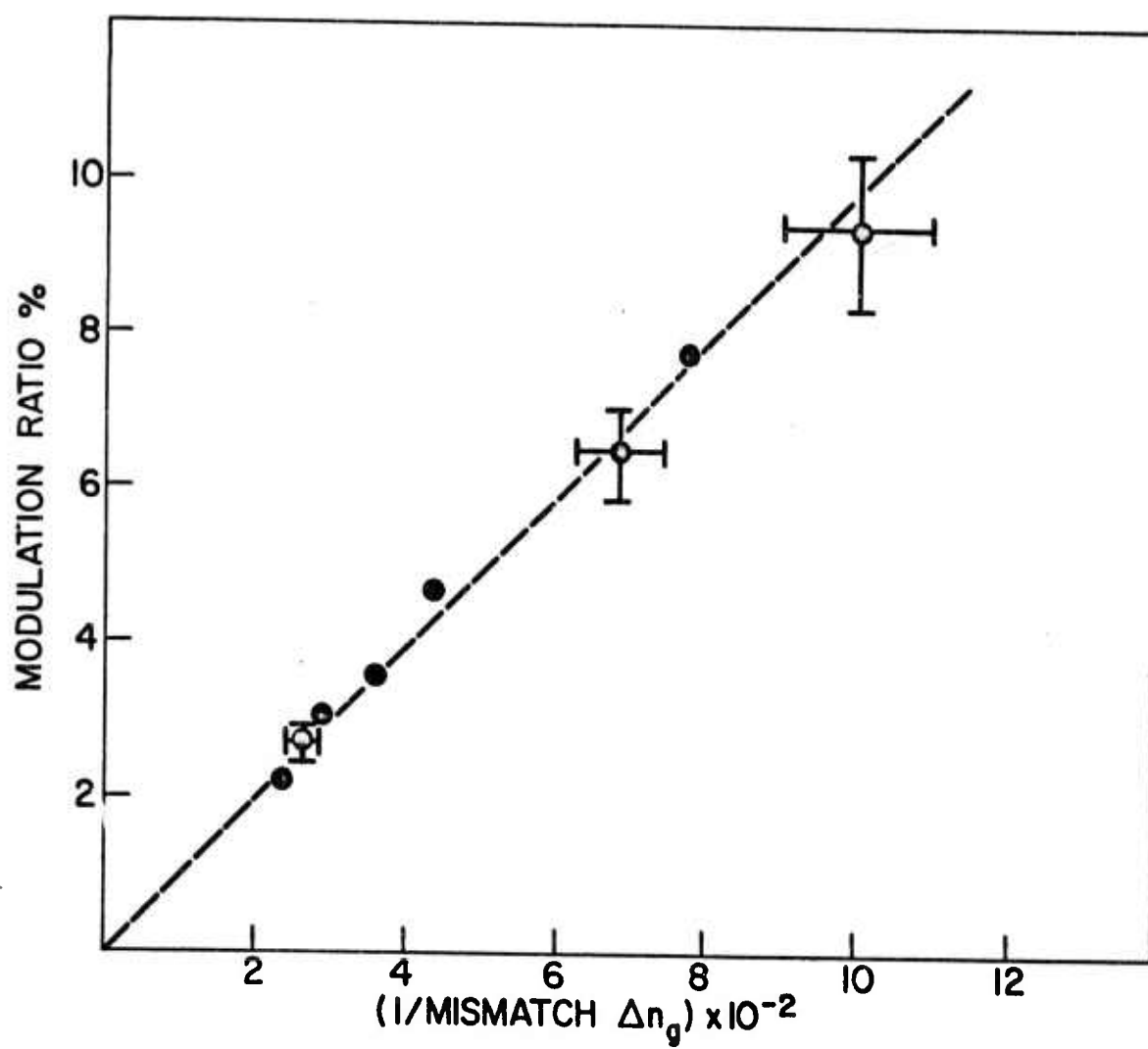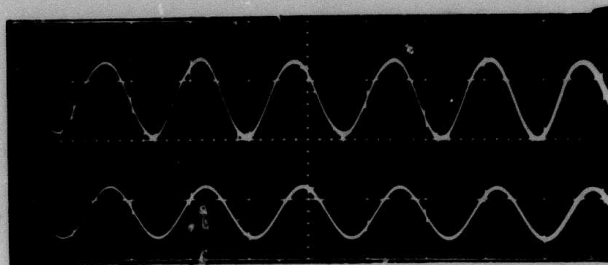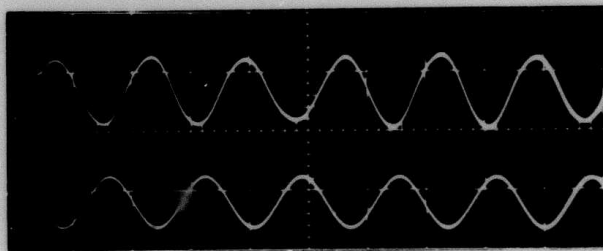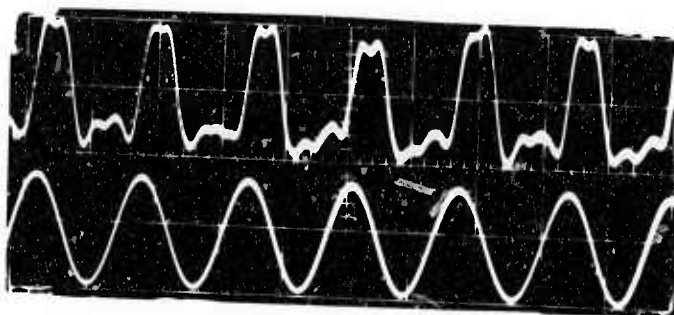
(b)
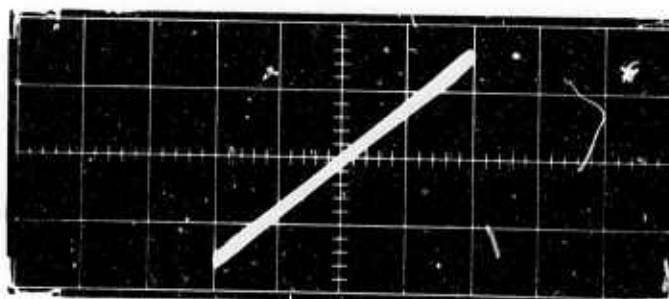
(c)
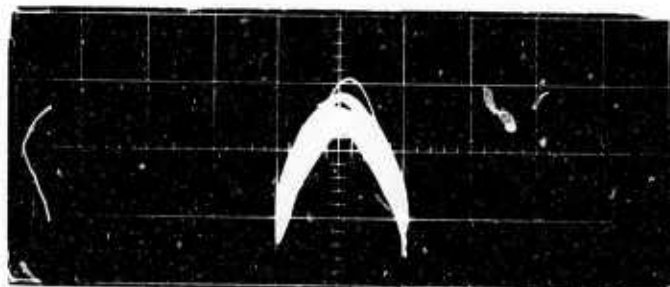
(a)

TE Modulation
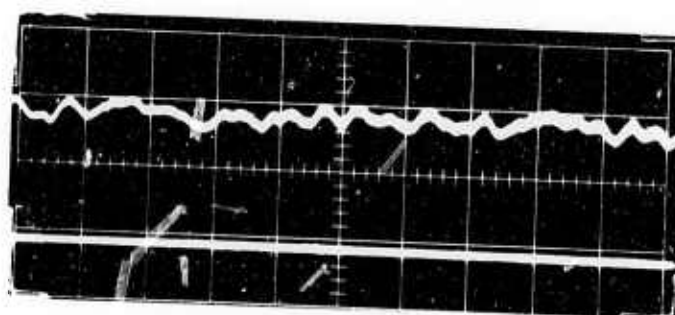

(b)
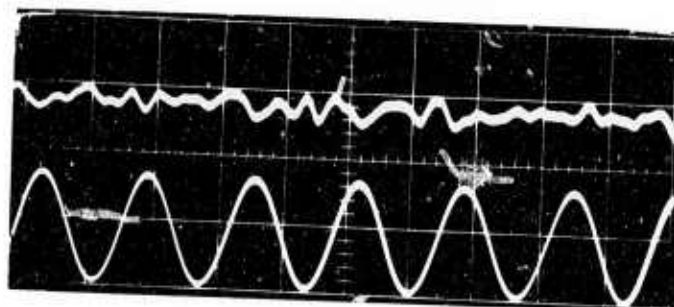
TM Modulation

(b)

(c)

V.   FINANCIAL STATEMENT

Contract N00014-73-C-0256

Total Contract Amount	Inception to Date Expenditures	Unexpended Funds
$99,000	$27,996.62	$71,003.38

Required Level of Effort	Inception to Date Level of Effort
4077 hrs.	1,340 hrs.

ACKNOWLEDGEMENT